Article:
Ning, Y. orcid.org/0000-0003-1808-3513, Han, L., Douverne, M. et al. (4 more authors) (2019) What dictates the spatial distribution of nanoparticles within calcite? Journal of the American Chemical Society, 141 (6). pp. 2481-2489. ISSN 0002-7863

https://doi.org/10.1021/jacs.8b12291

What Dictates the Spatial Distribution of Nanoparticles within Calcite?

Yin Ning,[*,†] Lijuan Han,[†] Marcel Douverne,[†] Nicholas J. W. Penfold,[†] Matthew J. Derry,[*,†] Fiona C. Meldrum,[‡] and Steven P. Armes[*,†]

[†] Department of Chemistry, University of Sheffield, Brook Hill, Sheffield, South Yorkshire S3 7HF, UK.

[‡] School of Chemistry, University of Leeds, Woodhouse Lane, Leeds, LS2 9JT, UK.

KEY WORDS: Polymerization-induced self-assembly (PISA), block copolymer vesicles, nanoparticle occlusion, small-angle X-ray scattering (SAXS), calcite ($CaCO_3$)

1. Experimental Section

1.1. Materials

Methacrylic acid (MAA), benzyl methacrylate (BzMA), fluorescein O-methacrylate (FMA, 97%), 4,4'-azobis(4-cyanovaleric acid) (ACVA; 99%), ammonium carbonate and calcium chloride hexahydrate were all purchased from Sigma-Aldrich (UK) and used as received. 4-Cyano-4-(2-phenylethane sulfanylthiocarbonyl)sulfanylpentanoic acid (PETTC) was prepared according to the protocol described by Semsarilar et al.[1] Deionized water was obtained from an in-house Elgastat Option 3A water purification unit. All solvents and reagents were obtained from Sigma-Aldrich (UK).

1.2. Synthesis of poly(methacrylic acid)$_{29}$ macro-CTA

A round-bottomed flask was charged with MAA (10.0 g; 116 mmol, target DP = 25), PETTC (1.58 g; 4.65mmol), ACVA (260.5 mg, 0.93 mmol, [PETTC]/[ACVA] = 5.0) and ethanol (15.0 g). The sealed reaction flask was purged with nitrogen and then immersed in a pre-heated oil bath at 70 °C for 3 h.

The MAA polymerization was quenched by cooling the flask in ice, followed by exposure of the reaction solution to air. The crude polymer was purified three times by precipitating into a ten-fold excess of diethyl ether. The resulting precipitate was redissolved in water and the final purified macro-CTA was obtained in powdered form by lyophilization (8.4 g; MAA conversion = 84%). A mean DP of 29 was calculated for this macro-CTA using ^{1}H NMR spectroscopy by comparing the integrated signal intensity assigned to the aromatic protons at 7.2-7.4 ppm with that due to the methacrylic backbone at 0.4-2.5 ppm. After exhaustive methylation using excess trimethylsilyldiazomethane in THF, THF GPC analysis indicated an M_n of 4,900 g mol^{-1} and an M_w/M_n of 1.21.

1.3. Synthesis of poly(methacrylic acid)$_{36}$ macro-CTA

A round-bottomed flask was charged with MAA (11.0 g; 128 mmol, target DP = 30), PETTC (1.45 g; 4.26mmol), ACVA (238.8 mg, 0.85 mmol, [PETTC]/[ACVA] = 5.0) and ethanol (16.5 g). The sealed reaction flask was purged with nitrogen and then immersed in a pre-heated oil bath at 70 °C for 3 h. The MAA polymerization was quenched by cooling the flask in ice, followed by exposure of the reaction solution to air. The crude polymer was purified three times by precipitating into a ten-fold excess of diethyl ether. The resulting precipitate was redissolved in water and the final purified macro-CTA was obtained in powdered form by lyophilization (7.8 g; MAA conversion = 78%). A mean DP of 36 was calculated for this macro-CTA using ^{1}H NMR spectroscopy by comparing the integrated signal intensity assigned to the aromatic protons at 7.2-7.4 ppm with that due to the methacrylic backbone at 0.4-2.5 ppm. After exhaustive methylation using excess trimethylsilyldiazomethane in THF, THF GPC analysis indicated an M_n of 5,400 g mol^{-1} and an M_w/M_n of 1.19.

1.4. Synthesis of poly(methacrylic acid)$_{54}$ macro-CTA

A round-bottomed flask was charged with MAA (12.25 g; 142 mmol, target DP = 50), PETTC (0.97 g; 2.85 mmol), ACVA (159.6 mg, 0.57 mmol, [PETTC]/[ACVA] = 5.0) and ethanol (18.38 g). The sealed reaction flask was purged with nitrogen and then immersed in a pre-heated oil bath at 70 °C for 3 h. The polymerization was quenched by cooling the flask in ice, followed by exposure of the reaction solution to air. The crude polymer was purified three times by precipitating into a ten-fold excess of diethyl ether. The resulting precipitate was redissolved in water and the final purified macro-CTA was obtained in powdered form by lyophilization (8.0 g; MAA conversion = 80%). A mean DP of 54 was calculated for this macro-CTA using ^{1}H NMR spectroscopy by comparing the integrated signal intensity assigned to the aromatic protons at 7.2-7.4 ppm with that due to the methacrylic backbone at 0.4-2.5 ppm. After exhaustive methylation using excess trimethylsilyldiazomethane in THF, THF GPC analysis indicated an M_n of 6,800 g mol^{-1} and an M_w/M_n of 1.22.

1.5. Synthesis of poly(methacrylic acid)$_{73}$ macro-CTA

A round-bottomed flask was charged with MAA (15.3 g; 178 mmol, target DP = 70), PETTC (0.864 g; 2.54 mmol), ACVA (142.4 mg, 0.508 mmol, [PETTC]/[ACVA] = 5.0) and ethanol (23.0 g). The sealed reaction flask was purged with nitrogen and immersed in a pre-heated oil bath at 70 °C for 3 h. The polymerization was quenched by cooling the flask in ice, followed by exposure of the reaction solution to air. The crude polymer was purified three times by precipitating into a ten-fold excess of diethyl ether. The precipitate was redissolved in water and the final purified macro-CTA was obtained in powdered form by lyophilization (11.5 g; MAA conversion = 75%). A mean DP of 73 was calculated for this macro-CTA using ^{1}H NMR spectroscopy by comparing the integrated signal intensity assigned to the aromatic protons at 7.2-7.4 ppm with that due to the methacrylic backbone at 0.4-2.5 ppm. After exhaustive methylation using excess trimethylsilyldiazomethane in THF, THF GPC analysis indicated an M_n of 8,700 g mol^{-1} and an M_w/M_n of 1.21.

1.6. Synthesis of poly(methacrylic acid)$_{29}$-poly(benzyl methacrylate)$_{200}$ (M_{29}-B_{200}) spheres

M_{29} macro-CTA (28.4 mg, 10.0 µmol), ACVA initiator (0.56 mg, 2.0 µmol, CTA/ACVA molar ratio = 5.0), FMA (2.0 mg, 5.0 µmol) and 75/25 w/w methanol/water (3.432 g) were weighed in turn into a 14 mL vial containing a magnetic stirrer bar. Then, benzyl methacrylate monomer (0.352 g, 2.0 mmol) was added to afford a 10 % w/w solution. The flask was sealed and degassed via N_2 for 30 min at 0 °C before being immersed in a 70 °C oil bath for 24 h. ^{1}H NMR analysis indicated more than 99% benzyl methacrylate conversion. The M_{29}-B_{200} spheres were purified by dialysis against water for one week using dialysis tubing with a molecular weight cut-off of 3,500 Da.

1.7. Synthesis of poly(methacrylic acid)$_{29}$-poly(benzyl methacrylate)$_{200}$ (M_{29}-B_{200}) vesicles

M_{29} macro-CTA (28.4 mg, 10.0 µmol), ACVA initiator (0.56 mg, 2.0 µmol, CTA/ACVA molar ratio = 5.0), FMA (2.0 mg, 5.0 µmol) and methanol (3.432 g) were weighed in turn into a 14 mL vial containing a magnetic stirrer bar. Benzyl methacrylate monomer (0.352 g, 2.0 mmol) was then added to afford a 10 % w/w solution. The flask was sealed and degassed via N_2 for 30 min at 0 °C before being immersed in a 70 °C oil bath for 24 h. ^{1}H NMR analysis indicated more than 99% benzyl methacrylate conversion. The M_{29}-B_{200} vesicles were diluted to 1.0 % w/w and then transferred into water by five centrifugation-redispersion cycles (30 min at 10,000 rpm for each cycle).

1.8. Synthesis of poly(methacrylic acid)$_{73}$-poly(benzyl methacrylate)$_{200}$ (M_{73}-B_{200}) spheres

M_{73} macro-CTA (66.2 mg, 10.0 µmol), ACVA initiator (0.56 mg, 2.0 µmol, CTA/ACVA molar ratio = 5.0), FMA (2.0 mg, 5.0 µmol) and 75/25 w/w methanol/water (3.773 g) were weighed in turn into a 14 mL vial containing a magnetic stirrer bar. Benzyl methacrylate monomer (0.352 g, 2.0 mmol) was then added to afford a 10 % w/w solution. The flask was sealed and degassed via N_2 for 30 min at 0 °C before being immersed in a 70 °C oil bath for 24 h. ^{1}H NMR analysis indicated more than 99%

benzyl methacrylate conversion. The M_{73}-B_{200} spheres were purified by dialysis against water for one week using dialysis tubing with a molecular weight cut-off of 3,500 Da.

1.9. Synthesis of poly(methacrylic acid)$_{73}$-poly(benzyl methacrylate)$_{200}$ (M_{73}-B_{200}) vesicles

M_{73} macro-CTA (66.2 mg, 10.0 µmol), ACVA initiator (0.56 mg, 2.0 µmol, CTA/ACVA molar ratio = 5.0), FMA (2.0 mg, 5.0 µmol) and 33/67 w/w methanol/ethanol (1.677 g) were weighed in turn into a 14 mL vial containing a magnetic stirrer bar. Benzyl methacrylate monomer (0.352 g, 2.0 mmol) was then added to afford a 20 % w/w solution. The flask was sealed and degassed via N_2 for 30 min at 0 °C before being immersed in a 70 °C oil bath for 24 h. ^{1}H NMR analysis indicated more than 99% benzyl methacrylate conversion. The M_{73}-B_{200} vesicles were diluted to 1.0 % w/w and then transferred into water via five centrifugation-redispersion cycles (30 min at 10,000 rpm for each cycle).

1.10. Synthesis of poly(methacrylic acid)$_{36}$-poly(benzyl methacrylate)$_{200}$ (M_{36}-B_{200}) vesicles

M_{36} macro-CTA (34.4 mg, 10.0 µmol), ACVA initiator (0.56 mg, 2.0 µmol, CTA/ACVA molar ratio = 5.0), FMA (2.0 mg, 5.0 µmol) and methanol (3.486 g) were weighed in turn into a 14 mL vial containing a magnetic stirrer bar. Benzyl methacrylate monomer (0.352 g, 2.0 mmol) was then added to afford a 10 % w/w solution. The flask was sealed and degassed via N_2 for 30 min at 0 °C before being immersed in a 70 °C oil bath for 24 h. ^{1}H NMR analysis indicated more than 99% benzyl methacrylate conversion. The M_{36}-B_{200} vesicles were diluted to 1.0 % w/w and then transferred in to water by five centrifugation-redispersion cycles (30 min at 10,000 rpm for each cycle).

1.11. Synthesis of poly(methacrylic acid)$_{54}$-poly(benzyl methacrylate)$_{200}$ (M_{54}-B_{200}) vesicles

M_{54} macro-CTA (49.9 mg, 10.0 µmol), ACVA initiator (0.56 mg, 2.0 µmol, CTA/ACVA molar ratio = 5.0), FMA (2.0 mg, 5.0 µmol) and 67/33 w/w methanol/ethanol (2.283 g) were weighed in turn into

a 14 mL vial containing a magnetic stirrer bar. Benzyl methacrylate monomer (0.352 g, 2.0 mmol) was then added to afford a 15 % w/w solids concentration. The flask was sealed and degassed via N_2 for 30 min at 0 °C before being immersed in a 70 °C oil bath for 24 h. ^{1}H NMR analysis indicated more than 99% benzyl methacrylate conversion. The M_{54}-B_{200} vesicles were diluted to 1.0 % w/w and then transferred into water via five centrifugation-redispersion cycles (30 min at 10,000 rpm for each cycle).

1.12. Precipitation of calcium carbonate crystals in the presence of various additives

An aqueous solution (10 mL) comprising $CaCl_2$ (1.5 mM) and 0.10 % w/w copolymer nanoparticles was placed in a dessicator. $CaCO_3$ crystals were precipitated onto a glass slide placed at the base of this aqueous solution by exposure to ammonium carbonate vapor (2-3 g, placed at the bottom of the dessicator) for 24 h at 20 ºC. Then the glass slide was removed from the solution and washed three times with deionized water followed by three rinses with ethanol. Each occlusion experiment was repeated at least twice and consistent results were obtained in each case.

2. Characterization

2.1. ^{1}H NMR spectroscopy

^{1}H NMR spectra were recorded using a Bruker Avance 400 spectrometer operating at 400 MHz using D_2O, CD_3OD or d_6-DMSO as solvents.

2.2. Gel permeation chromatography (GPC)

For THF GPC studies, the carboxylic acid groups on the $PMAA_x$ macro-CTA or $PMMA_x$-$PBzMA_y$ diblock copolymer were exhaustively methylated using trimethylsilyldiazomethane, as reported by Couvreur et al.[2] The GPC set-up comprised a HPLC pump and two 5 μM Mixed C columns connected

to a WellChrom K-2301 refractive index detector. The mobile phase was HPLC-grade THF containing 2% v/v triethylamine and 0.05% w/v butylhydroxytoluene (BHT) at a flow rate of 1.0 mL min^{-1}. Molecular weights are expressed relative to a series of near-monodisperse poly(methyl methacrylate) calibration standards.

2.3. Dynamic light scattering (DLS)

DLS measurements were conducted using a Malvern Zetasizer NanoZS instrument by detecting back-scattered light at an angle of 173°. Aqueous dispersions of the copolymer nanoparticles were diluted to 0.10 % w/v using deionized water. Aqueous electrophoresis measurements were conducted using disposable folded capillary cells supplied by Malvern (DTS1070) using the same instrument. For pH titration analyses, the nanoparticle concentration was fixed at 0.10 % w/w using 1 mM NaCl as background electrolyte. The solution pH was adjusted to pH 11 by addition of 0.5 NaOH and then manually reduced by addition of 0.01 M, 0.05 M or 0.10 M HCl. For [Ca^{2+}] titration analyses, the nanoparticle concentration was fixed at 0.10 % w/w and the [Ca^{2+}] was adjusted to 0, 0.05, 0.10, 0.25, 0.50, 1.00, 1.50, 3.00 or 6.00 mM at pH ~ 9.

2.4. Transmission electron microscopy (TEM)

TEM images were obtained by depositing droplets of 0.15 % w/v aqueous dispersion of copolymer nanoparticles onto carbon-coated palladium-copper grids (Agar Scientific, UK). Grids were treated with a plasma glow discharge for approximately 30 seconds to create a hydrophilic surface prior to addition of the aqueous nanoparticle dispersion (5 µL). Excess solvent was removed via blotting and each grid was stained with uranyl formate for 30 seconds. Excess stain was removed via blotting and each grid was carefully dried under vacuum. Imaging was performed using a FEI Tecnai G2 Spirit instrument operating at 80 keV.

2.5. Scanning electron microscopy (SEM)

Crystals were fractured by placing a clean glass slide on top of the calcite-coated glass slide, pressing down lightly and twisting one slide relative to the other. The resulting randomly-fractured calcite crystals were examined by scanning electron microscopy using an Inspect F instrument after sputter-coating with gold (15 mA, 1.5 min). To image the vesicles, one droplet of an aqueous dispersion of vesicles was dried onto a clean glass slide and then sputter-coated with gold prior to imaging.

2.6. Small angle X-ray scattering (SAXS)

SAXS patterns were recorded at a synchrotron source (ESRF, station ID02, Grenoble, France) using monochromatic X-ray radiation (X-ray wavelength $\lambda = 0.0995$ nm, scattering vector q ranging from 0.0015 to 0.15 $Å^{-1}$, where $q = 4\pi \sin\theta/\lambda$ and θ is one-half of the scattering angle) and a Ravonix MX-170HS CCD detector. A glass capillary of 2 mm diameter was used as a sample holder and measurements were conducted on 1.0% w/w aqueous dispersions. Scattering data were reduced and normalized with water being used for the absolute intensity calibration utilizing standard routines available at the beamline and were further analyzed using Irena SAS macros for Igor Pro.[3]

2.7. Other measurements

Optical microscopy images were recorded using a Motic DMBA300 digital biological microscope equipped with a built-in camera and analyzed using Motic Images Plus 2.0 ML software. Fluorescence microscopy images were recorded on a Zeiss Axio Scope A1 microscope fitted with an AxioCam 1Cm1 monochrome camera. Images were captured and processed using ZEN lite 2012 software. Confocal fluorescence images were recorded using a Nikon A1 microscope equipped with Nikon elements software. Raman spectra were recorded using a Renishaw 2000 Raman microscope equipped with a 785 nm diode laser. Thermogravimetric analysis (TGA) was conducted from 20 °C to 900 °C in air using a Perkin-Elmer Pyris 1 instrument at a heating rate of 10 °C min^{-1}.

SAXS Models

In general, the X-ray intensity scattered by a dispersion of particles [represented by the scattering cross section per unit sample volume, $\frac{d\Sigma}{d\Omega}(q)$] can be expressed as:

$$\frac{d\Sigma}{d\Omega}(q) = NS(q)\int_0^\infty \dots \int_0^\infty F\left(q, r_{1,} \dots, r_{\mathrm{k}}\right)^2 \Psi\left(r_{1,} \dots, r_{\mathrm{k}}\right) dr_1 \dots dr_{\mathrm{k}} \qquad \text{S1}$$

where $F(q, r_1, \dots, r_{\mathrm{k}})$ is their form factor, $r_1, \dots, r_{\mathrm{k}}$ is a set of k parameters describing the particle morphology, $\Psi\left(r_{1,} \dots, r_{\mathrm{k}}\right)$ is the distribution function, S(q) is the structure factor [generally, S(q) = 1 for dilute, non-interacting particles] and N is the particle number density per unit sample volume and is given by:

$$N = \frac{\varphi}{\int_0^\infty \dots \int_0^\infty V\left(r_{1,} \dots, r_{\mathrm{k}}\right) \Psi\left(r_{1,} \dots, r_{\mathrm{k}}\right) dr_1 \dots dr_{\mathrm{k}}} \qquad \text{S2}$$

where $V\left(r_{1,} \dots, r_{\mathrm{k}}\right)$ is the particle volume and φ is the particle volume fraction.

Spherical micelle model

The spherical micelle form factor for Equation S1 can be expressed as:[4]

$$\begin{aligned} F_{\mathrm{s\_mic}}(q) = {} & N_{\mathrm{s}}{}^2 \beta_{\mathrm{s}}{}^2 A_{\mathrm{s}}{}^2(q, R_{\mathrm{s}}) + N_{\mathrm{s}} \beta_{\mathrm{c}}{}^2 F_{\mathrm{c}}\left(q, R_{\mathrm{g}}\right) + N_{\mathrm{s}}(N_{\mathrm{s}} - 1) \beta_{\mathrm{c}}{}^2 A_{\mathrm{c}}{}^2(q) \\ & + 2N_{\mathrm{s}}{}^2 \beta_{\mathrm{s}} \beta_{\mathrm{c}} A_{\mathrm{s}}(q, R_{\mathrm{s}}) A_{\mathrm{c}}(q) \end{aligned} \qquad \text{S3}$$

where R_s is the radius of the spherical micelle core and R_g is the radius of gyration of the PMAA coronal block. The core block and the corona block X-ray scattering length contrast is given by $\beta_{\mathrm{s}} = V_{\mathrm{s}}(\xi_{\mathrm{s}} - \xi_{\mathrm{sol}})$ and $\beta_{\mathrm{c}} = V_{\mathrm{c}}(\xi_{\mathrm{c}} - \xi_{\mathrm{sol}})$, respectively. Here ξ_s, ξ_c and ξ_{sol} are the X-ray scattering length densities of the core block (ξ_{PBzMA} = 10.38 x 10^{10} cm^{-2}), the corona block (ξ_{PMAA} = 11.88 x 10^{10} cm^{-2}) and the solvent (for water, ξ_{sol} = 9.42 x 10^{10} cm^{-2}), respectively. V_s and V_c are the volumes of the core block (V_{PBzMA}) and the corona block (V_{PMAA}), respectively. These volumes were obtained from $V = \frac{M_{\mathrm{n,pol}}}{N_{\mathrm{A}}\rho}$ using the density of PBzMA (ρ_{PBzMA} = 1.15 g cm^{-3})[5] and PMAA (ρ_{PMAA} = 1.31 g cm^{-3}),[6] where $M_{n,pol}$ corresponds to the absolute number-average molecular weight of the block copolymer as determined by end-group analysis using ^{1}H NMR spectroscopy. The scattering amplitude of the micelle core is expressed via the sphere form factor amplitude:

$$A_s(q, R_s) = \Phi(qR_s)exp\left(-\frac{q^2\sigma^2}{2}\right) \quad \text{S4}$$

where $\Phi(qR_s) = \frac{3[\sin(qR_s) - qR_s\cos(qR_s)]}{(qR_s)^3}$. A sigmoidal interface between the two blocks is assumed for the spherical micelle form factor (Equation S4). This is described by the exponent term with a width σ accounting for a decaying scattering length density at the membrane surface. This σ value was fixed at 0.22 nm during fitting.

The scattering amplitude of the spherical micelle corona is:

$$A_c(q) = \Psi(qR_g)\left[\frac{sin(q[R_s + \delta R_g])}{q[R_s + \delta R_g]}\right] \quad \text{S5}$$

where $\Psi(qR_g) = \frac{1-exp(-qR_g)}{qR_g}$ and δ is the non-penetration depth of the corona chains into the core region, which was assumed to be equal to 1. The self-correlation term for the corona block is given by the Debye function:

$$F_c(q, R_g) = \frac{2[exp(-q^2{R_g}^2) - 1 + q^2{R_g}^2]}{q^4{R_g}^4} \quad \text{S6}$$

where R_g is the radius of gyration of the PMAA coronal block. The aggregation number, N_s, for spherical particles is given by:

$$N_s = (1 - x_{sol})\frac{\frac{4}{3}\pi{R_s}^3}{V_s} \quad \text{S7}$$

where x_{sol} is the volume fraction of solvent within the PBzMA cores. A polydispersity term for the core radius (R_s) was incorporated into the structural model (Equation S1) assuming a Gaussian distribution:

$$\Psi(r_1) = \frac{1}{\sqrt{2\pi{\sigma_{Rs}}^2}}exp\left(-\frac{(r_1 - R_s)^2}{2{\sigma_{Rs}}^2}\right) \quad \text{S8}$$

where σ_{Rs} is the standard deviation for R_s. In accordance with Equation S2, the number density per unit sample volume for the micelle model is expressed as:

$$N = \frac{\varphi}{\int_0^\infty V(r_1)\Psi(r_1)dr_1} \quad \text{S9}$$

where φ is the volume fraction of copolymer in a dispersion and $V(r_1)$ is the total volume of copolymer in a spherical micelle $[V(r_1) = (V_s + V_c)N_s(r_1)]$.

Vesicle model

The vesicle form factor in Equation S1 is expressed as:[7]

$$F_{ves}(q) = {N_v}^2{\beta_m}^2{A_m}^2(q) + N_v{\beta_{vc}}^2F_c(q, R_g) + N_v(N_v - 1){\beta_{vc}}^2{A_{vc}}^2(q) + 2{N_v}^2\beta_m\beta_{vc}A_m(q)A_{vc}(q) \quad \text{S10}$$

As in the spherical micelle model, the X-ray scattering length contrast for the membrane-forming block (PBzMA) and the coronal stabilizer block (PMAA) is given by $\beta_m = V_m(\xi_m - \xi_{sol})$ and $\beta_{vc} = V_{vc}(\xi_{vc} - \xi_{sol})$, respectively, where ξ_m, ξ_{vc} and ξ_{sol} are the X-ray scattering length densities of the membrane-forming block (ξ_{PBzMA} = 10.38 x 10^{10} cm^{-2}), the coronal stabilizer block (ξ_{PMAA} = 11.88 x 10^{10} cm^{-2}) and the solvent (ξ_{sol} = 9.42 x 10^{10} cm^{-2}). V_m and V_{vc} are the volumes of the membrane-forming block and the coronal stabilizer block, respectively. The volumes were calculated from $V = \frac{M_{n,pol}}{N_A\rho}$ using the density of PBzMA (ρ_{PBzMA} = 1.15 g cm^{-3})[5] and the density of PMAA (ρ_{PMAA} = 1.31 g cm^{-3})[6], where $M_{n,pol}$ corresponds to the number-average molecular weight of the block copolymer as determined by ^{1}H NMR spectroscopy. The amplitude of the membrane self-term is:

$$A_m(q) = \frac{V_{out}\varphi(qR_{out}) - V_{in}\varphi(qR_{in})}{V_{out} - V_{in}} exp\left(-\frac{q^2{\sigma_{in}}^2}{2}\right) \quad \text{S11}$$

where $R_{in} = R_m - \frac{1}{2}T_m$ is the inner radius of the membrane, $R_{out} = R_m + \frac{1}{2}T_m$ is the outer radius of the membrane, $V_{in} = \frac{4}{3}\pi{R_{in}}^3$ and $V_{out} = \frac{4}{3}\pi{R_{out}}^3$. It should be noted that Equation S10 differs from the original work in which they were first reported.[7] The exponent term in Equation S11 represents a

sigmoidal interface between the blocks, with a width σ_{in} accounting for a decaying scattering length density at the membrane surface. The numerical value for σ_{in} was fixed at 2.5. The mean vesicle aggregation number, N_v, is given by:

$$N_{\mathrm{v}} = (1 - x_{\mathrm{sol}})\frac{V_{\mathrm{out}} - V_{\mathrm{in}}}{V_{\mathrm{m}}} \qquad \text{S12}$$

where x_{sol} is the solvent (i.e. water) volume fraction within the vesicle membrane. Assuming that there is no penetration of the solvophilic coronal blocks into the solvophobic membrane, the amplitude of the vesicle corona self-term is given by:

$$A_{\mathrm{vc}}(q) = \Psi(qR_{\mathrm{g}})\frac{1}{2}\left[\frac{sin\left[q\left(R_{\mathrm{out}} + R_{\mathrm{g}}\right)\right]}{q\left(R_{\mathrm{out}} + R_{\mathrm{g}}\right)} + \frac{sin\left[q\left(R_{\mathrm{in}} - R_{\mathrm{g}}\right)\right]}{q\left(R_{\mathrm{in}} - R_{\mathrm{g}}\right)}\right] \qquad \text{S13}$$

For this vesicle model it is assumed that both the overall vesicle radius and the vesicle membrane thickness (R_m and T_m, respectively) have an associated Gaussian distribution. Hence the polydispersity function in Equation S1 can be expressed as:

$$\Psi(r_1, r_2) = \frac{1}{\sqrt{2\pi{\sigma_{R\mathrm{m}}}^2}} exp\left(-\frac{(r_1 - R_{\mathrm{m}})^2}{2{\sigma_{R\mathrm{m}}}^2}\right)\frac{1}{\sqrt{2\pi{\sigma_{T\mathrm{m}}}^2}} exp\left(-\frac{(r_2 - T_{\mathrm{m}})^2}{2{\sigma_{T\mathrm{m}}}^2}\right) \qquad \text{S14}$$

where σ_{Rm} and σ_{Tm} are the standard deviations for R_m and T_m, respectively. Following Equation S2, the number density per unit volume for the vesicle model is expressed as:

$$N = \frac{\varphi}{\int_0^\infty \int_0^\infty V(r_1, r_2)\Psi(r_1, r_2)dr_1 dr_2} \qquad \text{S15}$$

where φ is the total volume fraction of copolymer self-assembled into vesicles and $V(r_1, r_2)$ is the total volume of copolymer in a vesicle $[V(r_1, r_2) = (V_{\mathrm{m}} + V_{\mathrm{vc}})N_{\mathrm{v}}(r_1, r_2)]$.

Spherical micelle, dimer and trimer model

In order to achieve a satisfactory fit for the $PMAA_{73}$-$PBzMA_{200}$ nanoparticles, it was necessary to consider the coexistence of spherical micelles together with dimer and trimer assemblies. The contribution to the overall scattering intensity of the spherical micelles is represented by the form factor, $F_{\mathrm{s\_mic}}(q)$, described in Equation S3. A formalism used for the scattering intensity of interacting micelles:[8]

$$I = F_{\mathrm{s\_mic}}(q) + F^{\mathrm{av}}_{\mathrm{s\_mic}}(q)[S(q) - 1] \qquad \text{S16}$$

was applied to derive form factors of both micelle dimers and micelle trimers. Thus the relative scattering intensity of a mixture of unimer micelles, dimer micelles and trimer micelles can be expressed as:

$$I = F_{\mathrm{s\_mic}}(q)\sum_{n=1}^{3} k_{\mathrm{n}} + F^{\mathrm{av}}_{\mathrm{s\_mic}}(q)\sum_{n=2}^{3} nk_{\mathrm{n}}\,[S(q) - 1] \qquad \text{S17}$$

where n is the number of spheres forming unimers, dimers or trimers, and k_n is the volume fraction of each nano-object, $k_1 + k_2 + k_3 = 1$. The form factor for the average radial scattering length density distribution of spherical micelles indicated in both Equation S16 and Equation S17 is given by:

$$F^{\mathrm{av}}_{\mathrm{s_{mic}}}(q) = {N_{\mathrm{s}}}^2{\beta_{\mathrm{s}}}^2{A_{\mathrm{s}}}^2(q, R_{\mathrm{s}}) + N_{\mathrm{s}}(N_{\mathrm{s}} - 1){\beta_{\mathrm{c}}}^2{A_{\mathrm{c}}}^2(q) + 2{N_{\mathrm{s}}}^2\beta_{\mathrm{s}}\beta_{\mathrm{c}}A_{\mathrm{s}}(q, R_{\mathrm{s}})A_{\mathrm{c}}(q) \qquad \text{S18}$$

The form factor for both dimer micelles and trimer micelles (Equation S17) includes the Debye equation:[9]

$$S_{\mathrm{n}}(q) = 1 + \frac{2}{n}\sum_{i=1}^{n-1}\sum_{j=i+1}^{n}\frac{sin(qr_{ij})}{qr_{ij}} \qquad \text{S19}$$

where the inter-micelle separation distances are $r_{12} = r_{23} = 2(R_s+R_g)$ and $r_{13} = 4(R_s + R_g)$. Due to possible interpenetration of the coronal chains on adjacent micelles, R_g (rather than $2R_g$) is used in the expressions for the inter-micelle separation distances. The size dispersity of the micelles was determined assuming a normal distribution of the core radius (R_s).

Calculation of the mean aggregation number (N_{agg}) and the number of copolymer chains per unit surface area (S_{agg}), otherwise known as the stabilizer surface density

For simplicity, the number of copolymer chains per nanoparticle (or mean aggregation number) is termed N_{agg} regardless of the copolymer morphology. For spherical nanoparticles, $N_{agg} = N_s$ (see Equation S7 above), whereas for vesicles, $N_{agg} = N_v$ (see Equation S12 above). In all cases, the solvent volume fraction within the PBzMA block (x_{sol}) was assumed to be zero.

Similarly, the number of copolymer chains per unit surface area is termed S_{agg} regardless of the copolymer morphology. For spherical nanoparticles, the following equation was used:

$$S_{\text{agg}} = \frac{N_{\text{s}}}{4\pi {R_{\text{s}}}^2} \qquad \text{S20}$$

For vesicles, the corresponding equation is:

$$S_{\text{agg}} = \frac{N_{\text{v}}}{4\pi\left({R_{\text{out}}}^2 + {R_{\text{in}}}^2\right)} \qquad \text{S21}$$

Table S1. Summary of Synthesis Parameters for the M_x-B_{200} Diblock Copolymer Nanoparticles

Copolymer ID	Macro-CTA		BzMA		FMA		[macro-CTA]/ [initiator] molar ratio	Solvent composition		Copolymer concentration % w/w
	mass (mg)	moles (µmol)	mass (g)	moles (mmol)	mass (mg)	moles (µmol)		Solvent(s)	mass (g)	
M_{29}-B_{200} (S)	28.4	10.0	0.352	2.0	2.0	5.0	5.0	75/25 w/w methanol/water	3.432	10
M_{73}-B_{200} (S)	66.2	10.0	0.352	2.0	2.0	5.0	5.0	75/25 w/w methanol/water	3.773	10
M_{29}-B_{200} (V)	28.4	10.0	0.352	2.0	2.0	5.0	5.0	methanol	3.432	10
M_{36}-B_{200} (V)	34.4	10.0	0.352	2.0	2.0	5.0	5.0	methanol	3.486	10
M_{54}-B_{200} (V)	49.9	10.0	0.352	2.0	2.0	5.0	5.0	67/33 w/w methanol/ethanol	2.283	15
M_{73}-B_{200} (V)	66.2	10.0	0.352	2.0	2.0	5.0	5.0	33/67 w/w methanol/ethanol	1.677	20

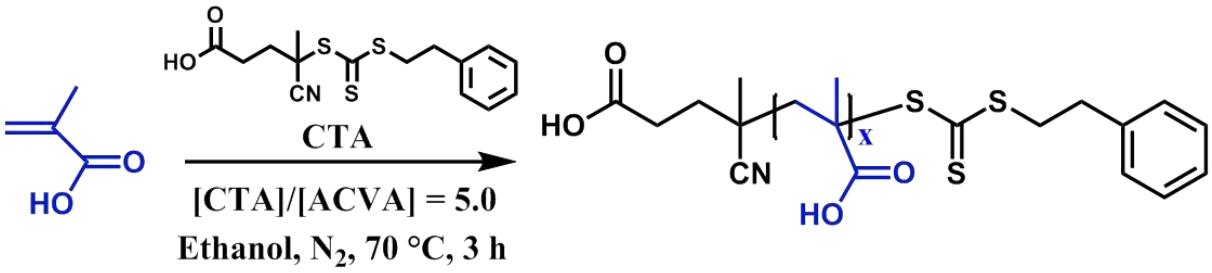

Scheme S1. Synthesis of poly(methacrylic acid) macro-CTAs via RAFT solution polymerization.

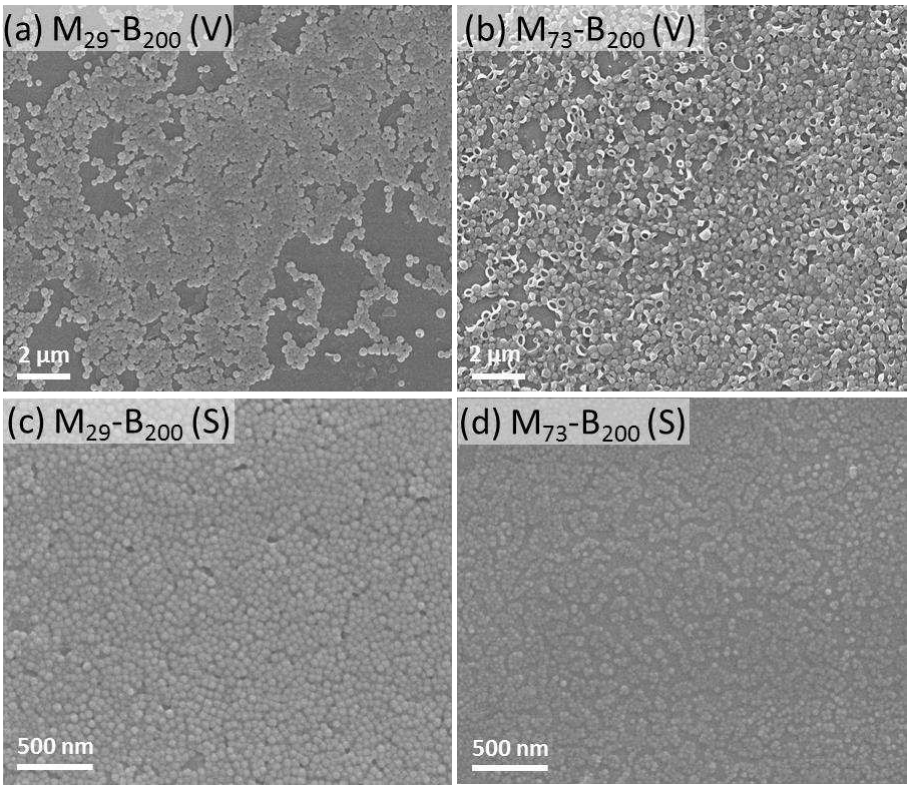

Figure S1. Representative SEM images recorded for various anionic poly(methacrylic acid)-poly(benzyl methacrylate) diblock copolymer nanoparticles (either vesicles or spheres) prepared via RAFT dispersion polymerization of benzyl methacrylate. (a) M_{29}-B_{200} vesicles; (b) M_{73}-B_{200} vesicles; (c) M_{29}-B_{200} spheres and (d) M_{73}-B_{200} spheres.

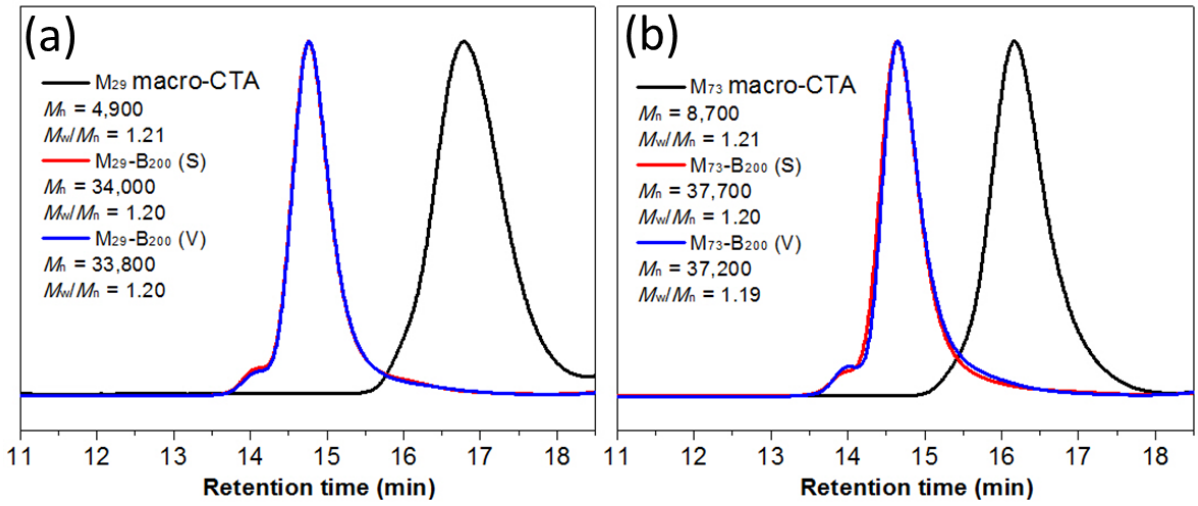

Figure S2. THF GPC curves (vs. poly(methyl methacrylate) calibration standards) recorded for methylated M_x macro-CTAs and their corresponding methylated M_x-B_y diblock copolymers. In each case, the methacrylic acid residues were methylated using excess trimethylsilyldiazomethane. According to these GPC curves, high blocking efficiencies were obtained when chain-extending each macro-CTA with benzyl methacrylate. Meanwhile, the GPC curves obtained for the two methylated M_{29}-B_{200} diblock copolymers and the two methylated M_{73}-B_{200} diblock copolymers overlap almost perfectly. This means that essentially the same copolymer chains can self-assemble to form either kinetically-trapped spheres or vesicles depending on the reaction conditions employed for the PISA synthesis (e.g. the solvent composition and copolymer concentration, see **Table S1**).

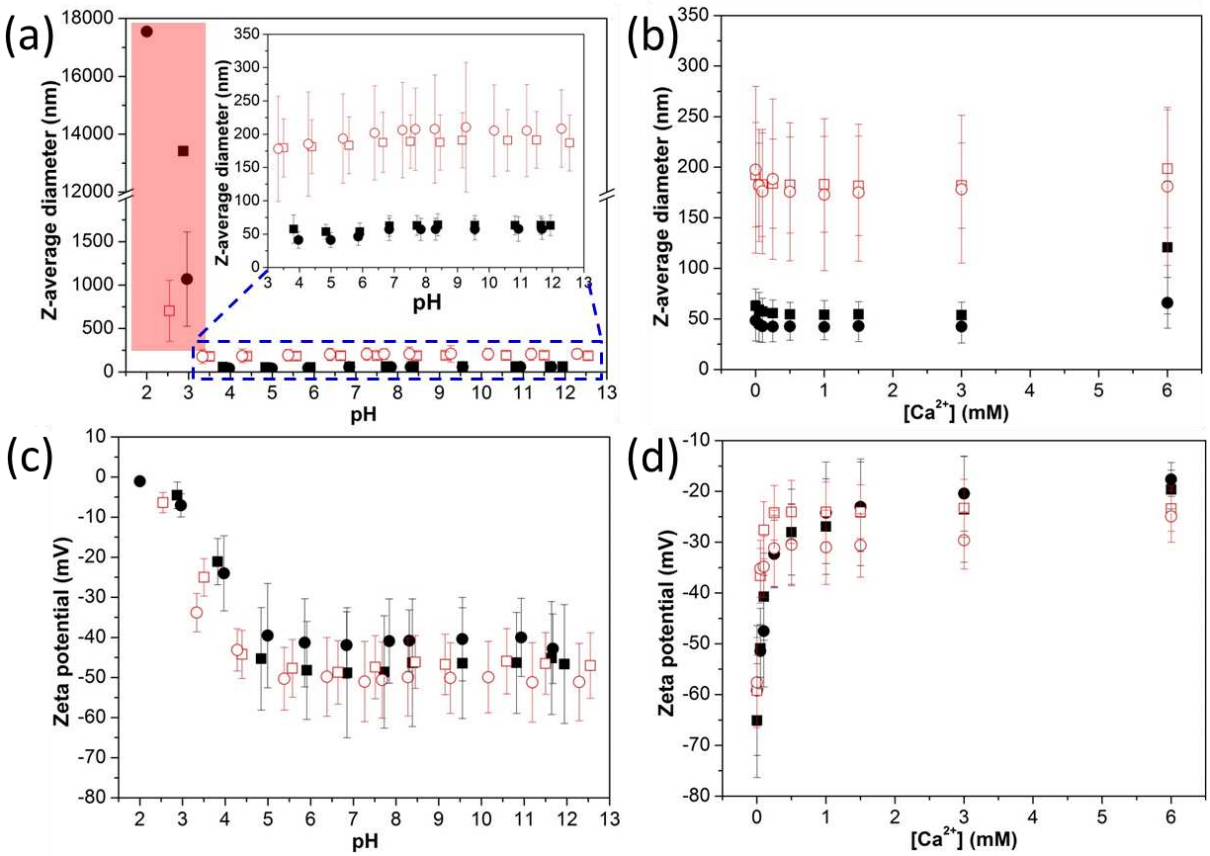

Figure S3. Characterization of various diblock copolymer nanoparticles by dynamic light scattering (DLS) and aqueous electrophoresis. (a) Z-average diameter vs. pH; the larger diameters within the pink rectangle indicate nanoparticle aggregation while the inset shows more clearly the data within the dotted blue rectangle; (b) z-average diameter vs. Ca^{2+} concentration; (c) zeta potential vs. pH; (d) zeta potential vs. Ca^{2+} concentration. Open squares (□) and filled squares (■) represent M_{29}-B_{200} vesicles and M_{29}-B_{200} spheres, respectively; open circles (○) and filled squares (●) represent M_{73}-B_{200} vesicles and M_{73}-B_{200} spheres, respectively.

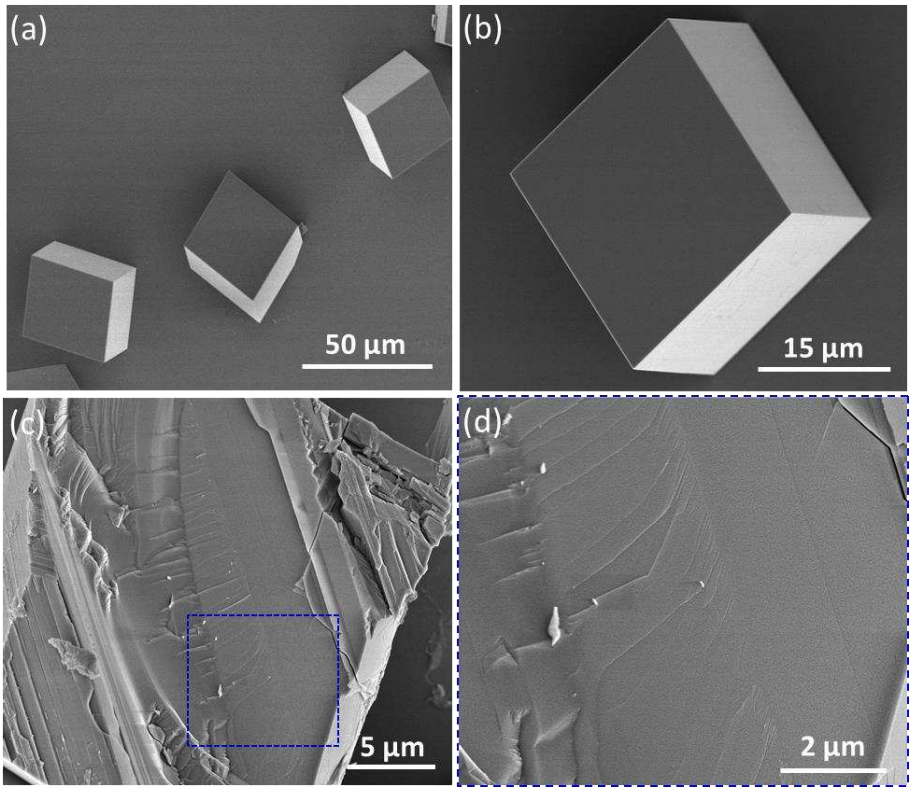

Figure S4. SEM images of calcite crystals precipitated in the absence of any additives (control experiments): (a) low magnification image showing several crystals; (b) an individual calcite crystal; (c) internal structure of a randomly-fractured calcite crystal; (d) higher magnification image showing the featureless area indicated in (c).

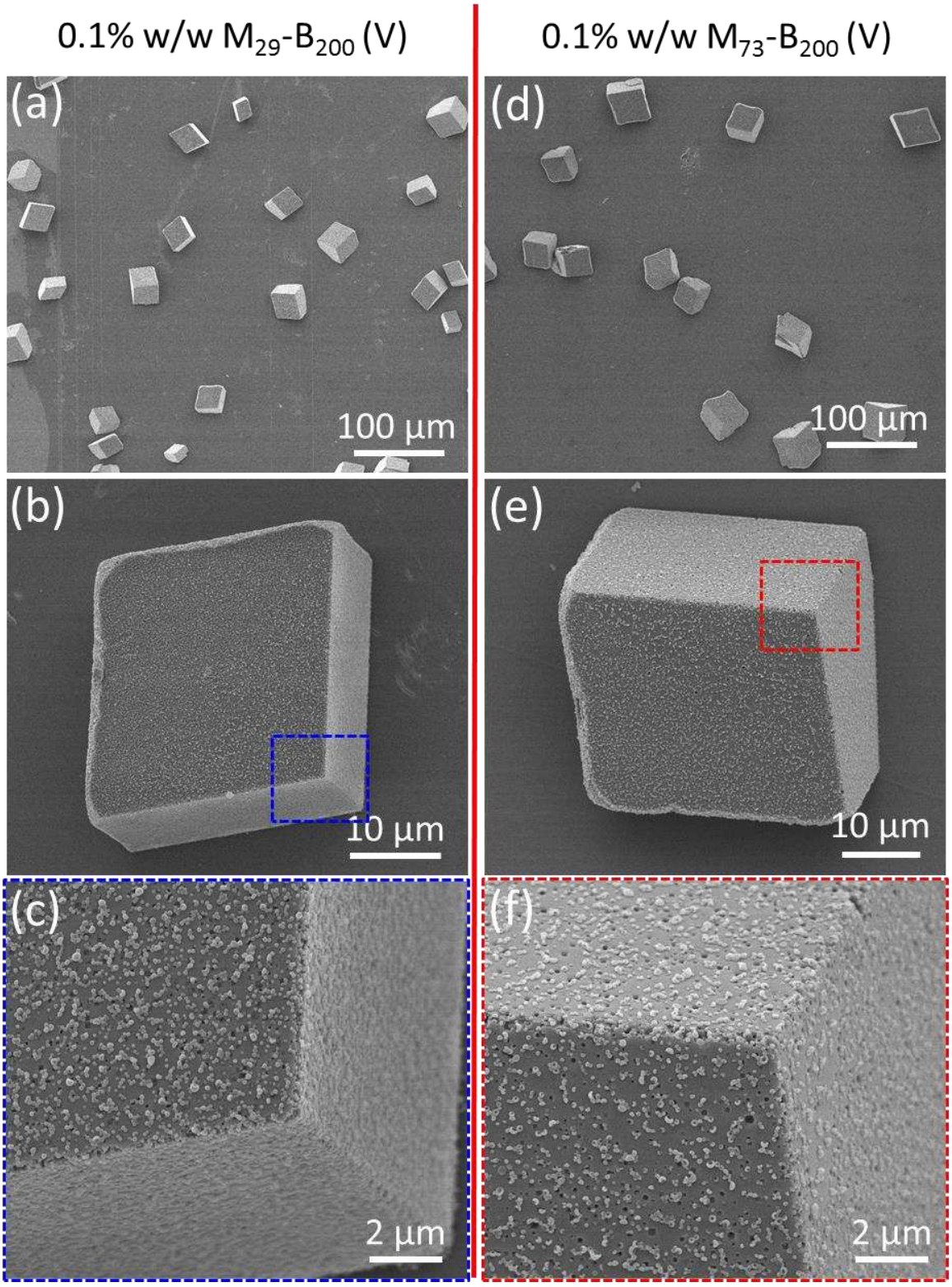

Figure S5. Calcite crystals precipitated in the presence of (a, b, c): 0.1% w/w M_{29}-B_{200} vesicles or (d, e, f): 0.1% w/w M_{73}-B_{200} vesicles.

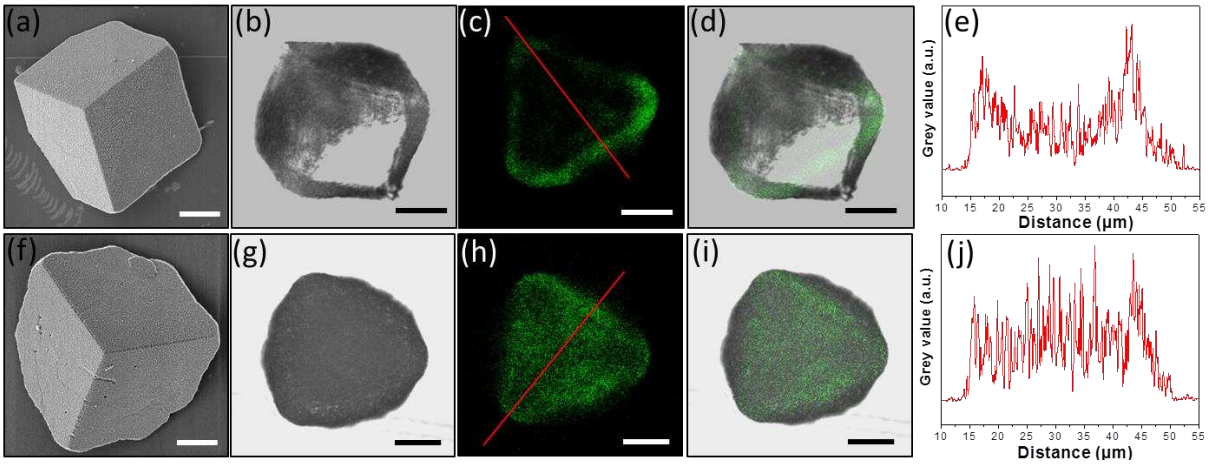

Figure S6. Spatial distribution of (a-e) M_{29}-B_{200} vesicles and (f-j) M_{73}-B_{200} vesicles occluded within calcite crystals. (a) and (f) are representative SEM images; (b) and (g) are representative optical micrographs; (c) and (h) are representative confocal fluorescence micrographs; (d) and (i) are merged micrographs; (e) and (j) are line profiles, calculated from the red lines indicated in (c) and (h), respectively. All scale bars correspond to 10 μm. N.B. These calcite crystals were intentionally imaged with one apex face-up because the highest resolution can be obtained under such conditions.

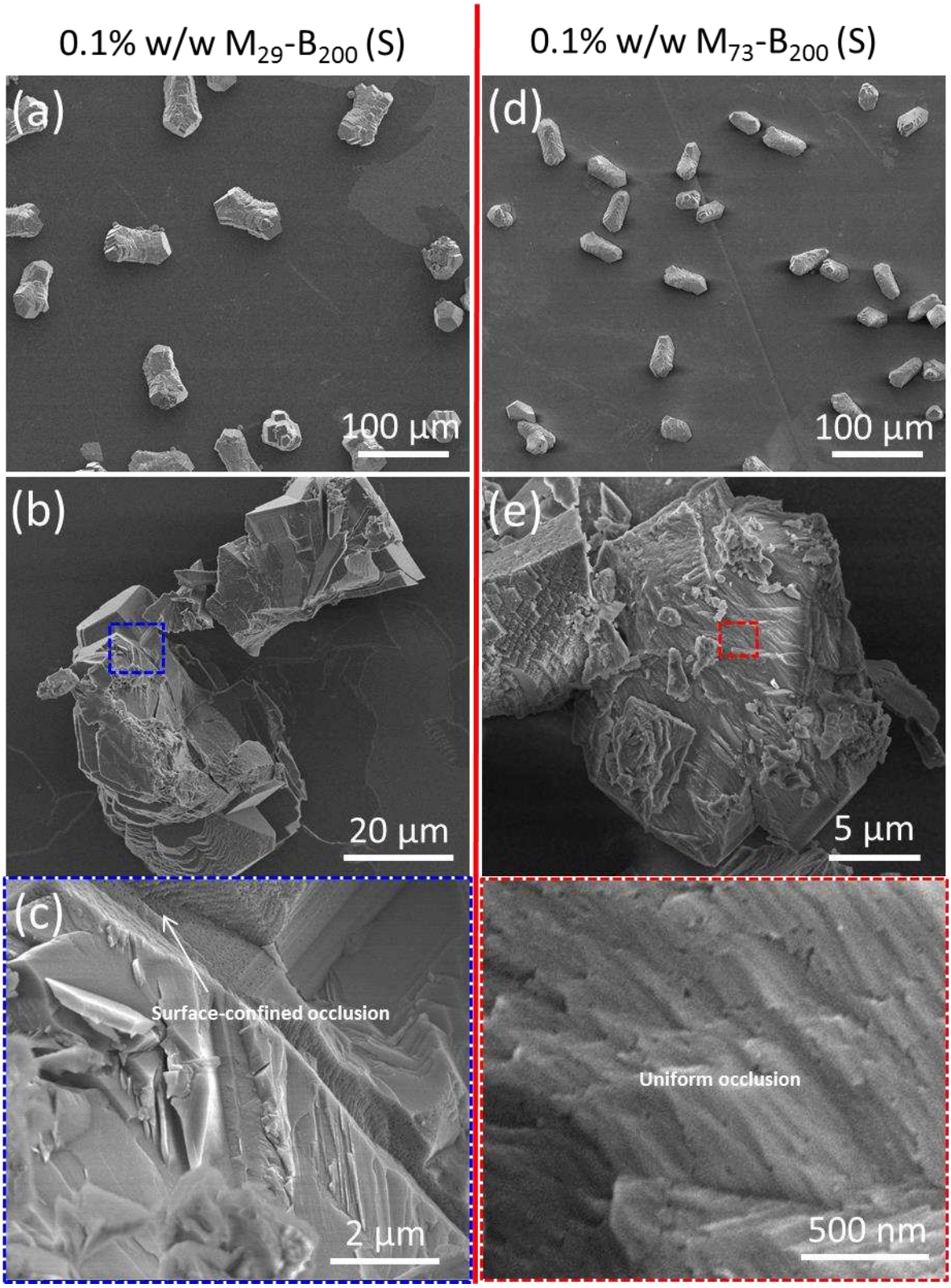

Figure S7. Calcite crystals precipitated in the presence of (a, b, c) 0.1% w/w M_{29}-B_{200} spheres and (d, e, f) 0.1% w/w M_{73}-B_{200} spheres.

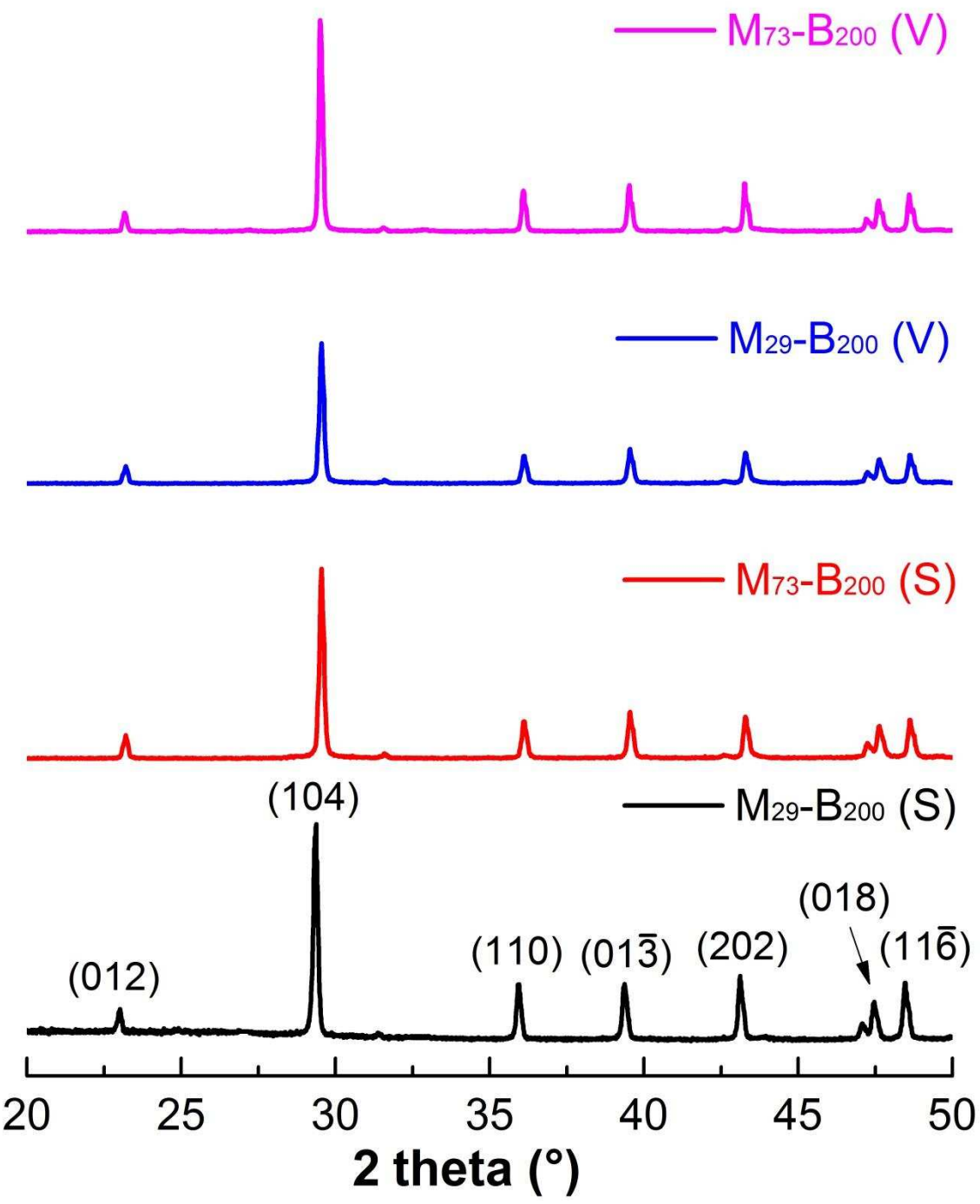

Figure S8. Powder XRD spectra recorded for calcite crystals precipitated in the presence of the following anionic diblock copolymer nano-objects: M_{29}-B_{200} spheres, M_{73}-B_{200} spheres, M_{29}-B_{200} vesicles and M_{73}-B_{200} vesicles.

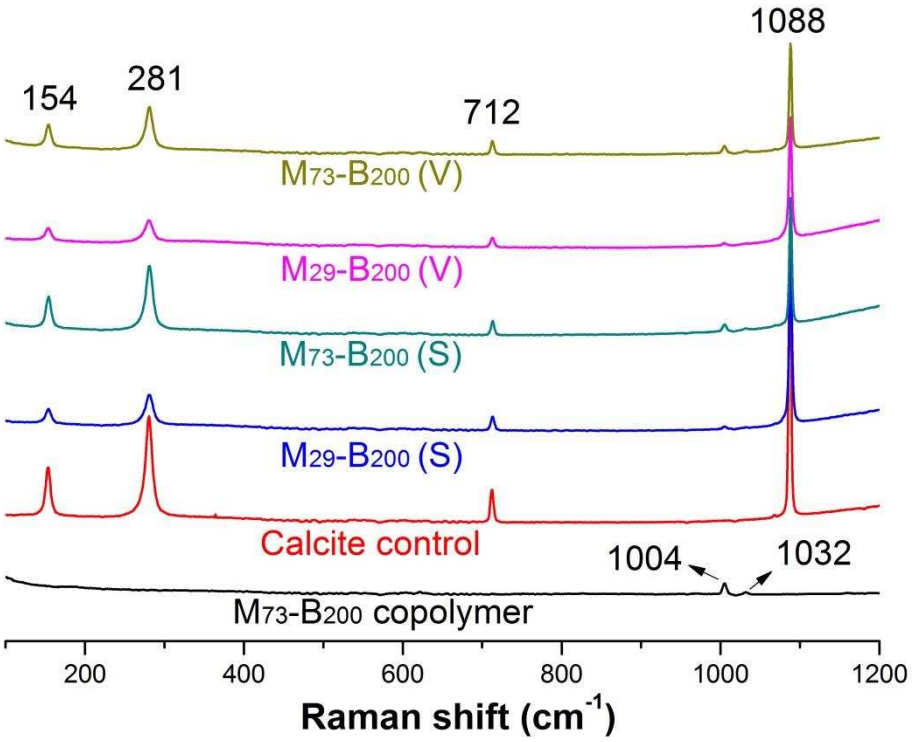

Figure S9. Raman spectra recorded for M_{73}-B_{200} copolymer, a pure calcite control, and calcite crystals prepared in the presence of M_{29}-B_{200} spheres, M_{73}-B_{200} spheres, M_{29}-B_{200} vesicles and M_{73}-B_{200} vesicles.

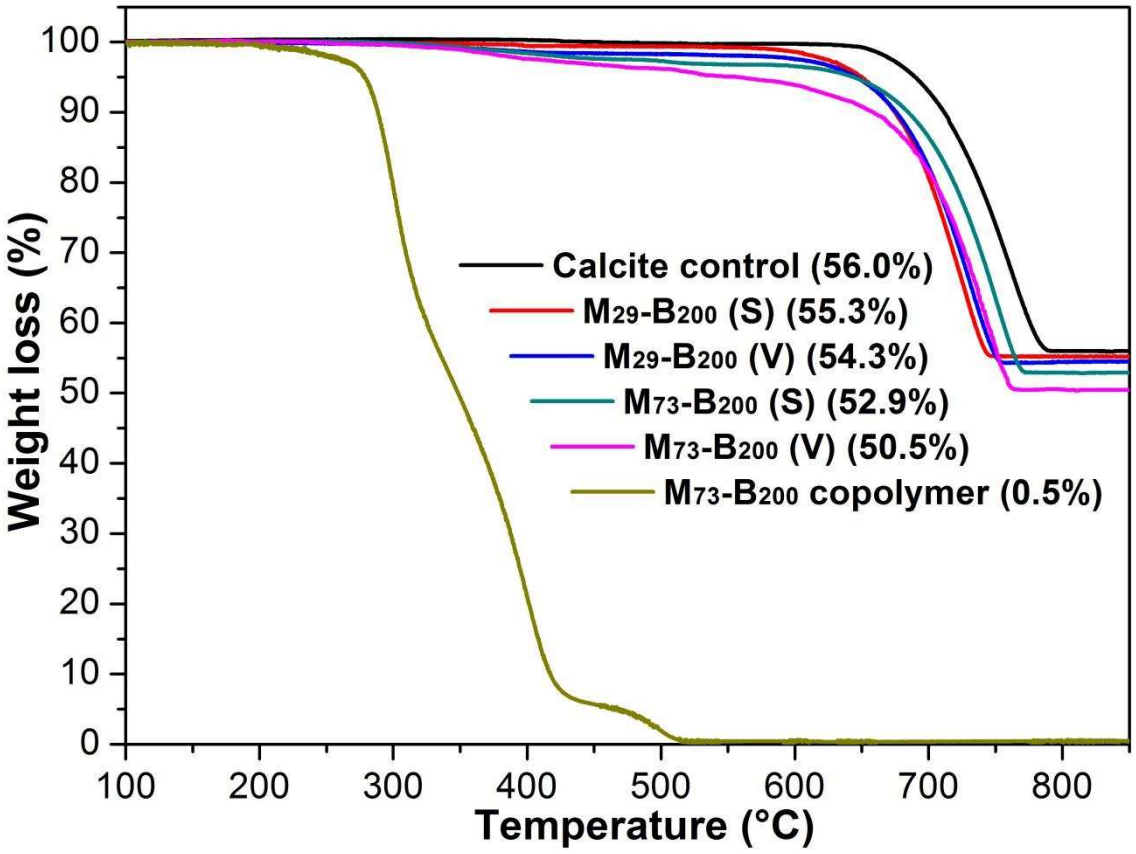

Figure S10. Thermogravimetric analysis (TGA) curves recorded for a pure calcite control, M_{29}-B_{200} spheres in calcite, M_{29}-B_{200} vesicles in calcite, M_{73}-B_{200} spheres in calcite, M_{73}-B_{200} vesicles in calcite and M_{73}-B_{200} copolymer alone. Detailed calculations for the extent of occlusion from such TGA data can be found in our previous publication.[10]

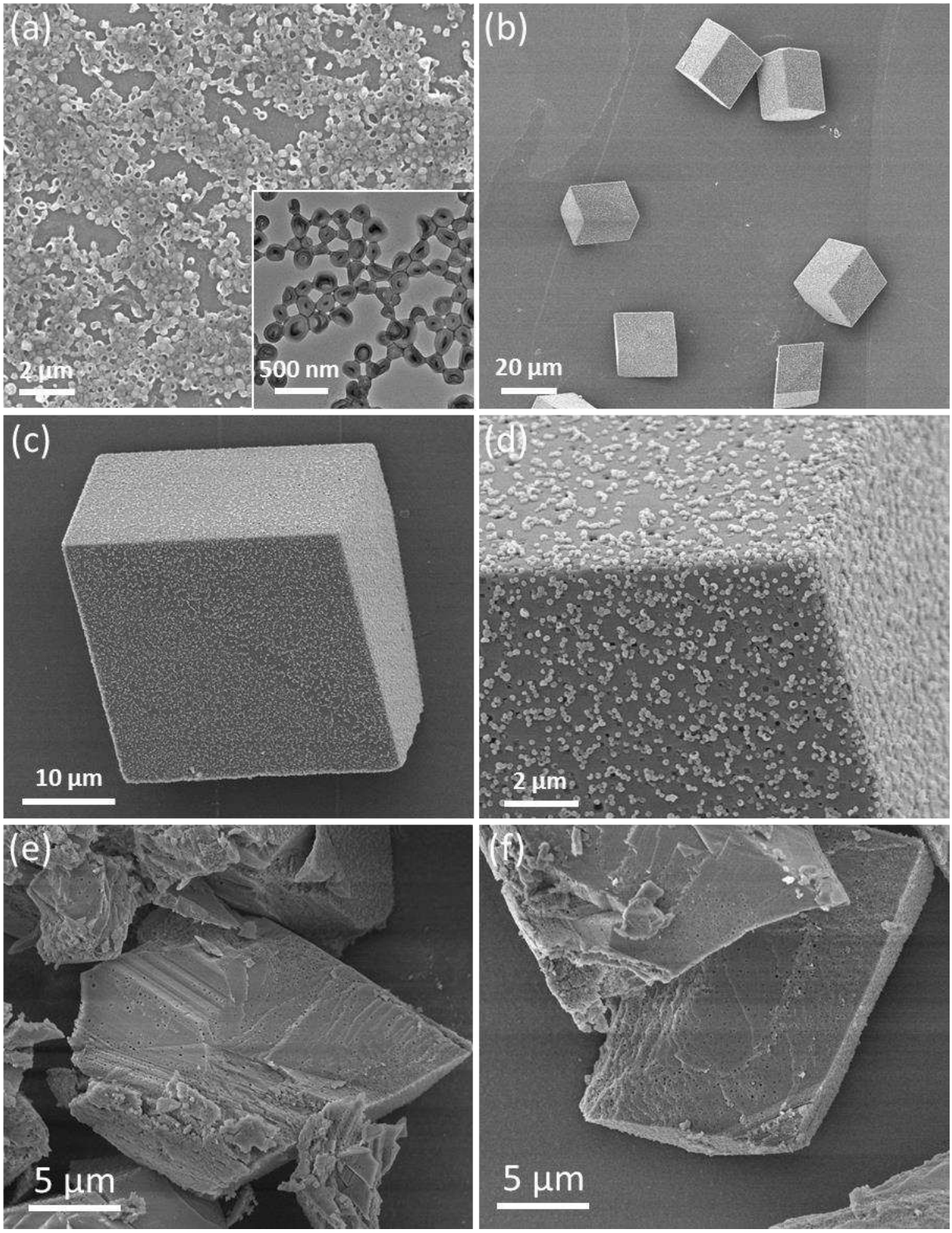

Figure S11. Calcite crystals prepared in the presence of 0.1% w/w M_{36}-B_{200} vesicles. (a) SEM image recorded for M_{36}-B_{200} vesicles with the inset showing the corresponding TEM image; (b) low magnification SEM image of calcite crystals precipitated in the presence of 0.1% w/w M_{36}-B_{200} vesicles; (c) higher magnification SEM image of an individual crystal; (d) SEM image showing the surface structure of this crystal; (e) and (f) SEM images of randomly-fractured calcite crystals, showing that vesicle occlusion is non-uniform in this case.

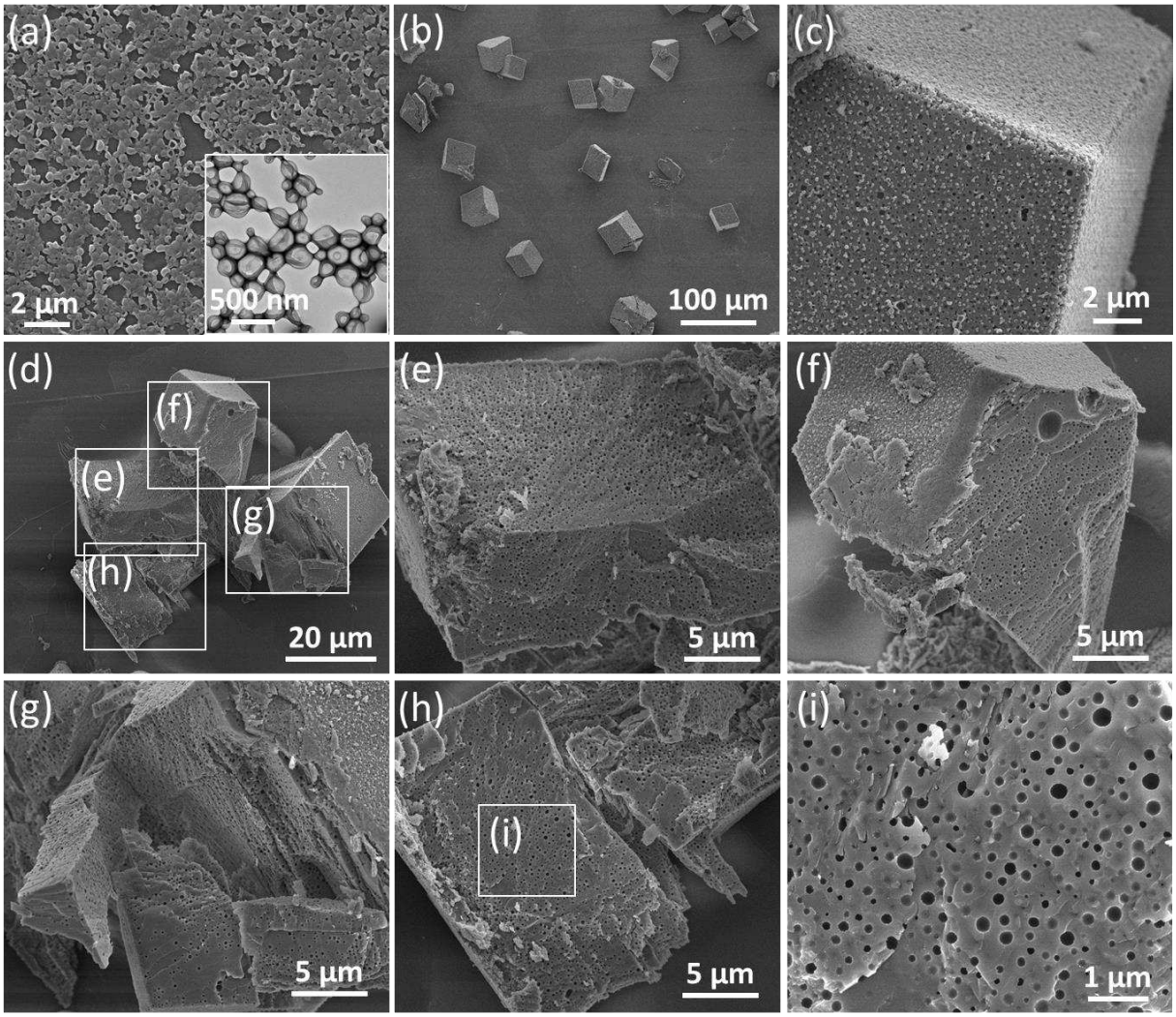

Figure S12. Calcite crystals prepared in the presence of 0.1% w/w M_{54}-B_{200} vesicles. (a) SEM image recorded for M_{54}-B_{200} vesicles with the inset showing the corresponding TEM image; (b) low magnification SEM image of intact $CaCO_3$ crystals prepared in the presence of 0.1% w/w M_{54}-B_{200} vesicles; (c) higher magnification SEM showing the surface structure of an individual crystal; (d) a randomly-fractured crystal; (e)-(h) higher magnification SEM images of the areas indicated in (d); (i) higher magnification SEM image of the area indicated in (h). Images (d)-(i) confirm that these M_{54}-B_{200} vesicles are uniformly occluded within calcite. The corresponding TGA data indicates that the extent of vesicle occlusion is 8.65% by mass, which is slightly lower than that obtained for the M_{73}-B_{200} vesicles (9.91% by mass).

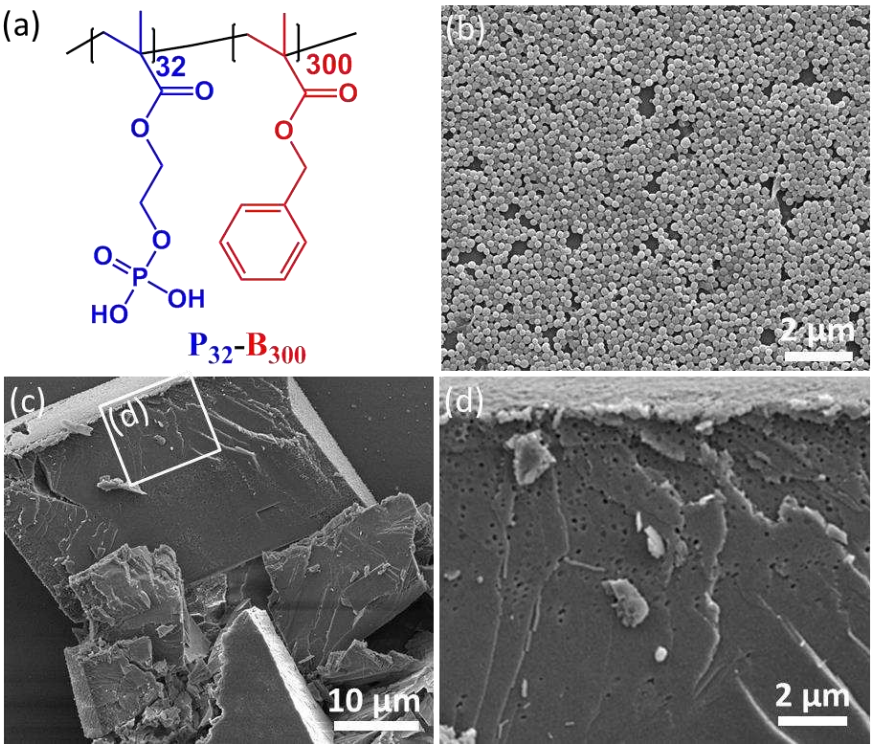

Figure S13. Occlusion of poly(2-(phosphonooxy)ethyl methacrylate)$_{32}$-poly(benzyl methacrylate)$_{300}$ (P_{32}-B_{300}) diblock copolymer nanoparticles within calcite crystals. (a) Chemical structure of P_{32}-B_{300} diblock copolymer nanoparticles; (b) SEM image recorded for P_{32}-B_{300} diblock copolymer nanoparticles; (c) SEM image showing the internal structure of a randomly-fractured calcite crystal prepared in the presence of 0.1% w/w P_{32}-B_{300} diblock copolymer nanoparticles; (d) magnified SEM image, showing the area indicated in (c). Clearly, occlusion of the P_{32}-B_{300} diblock copolymer nanoparticles is non-uniform, with the majority of the occluded nanoparticles being confined within a surface layer.

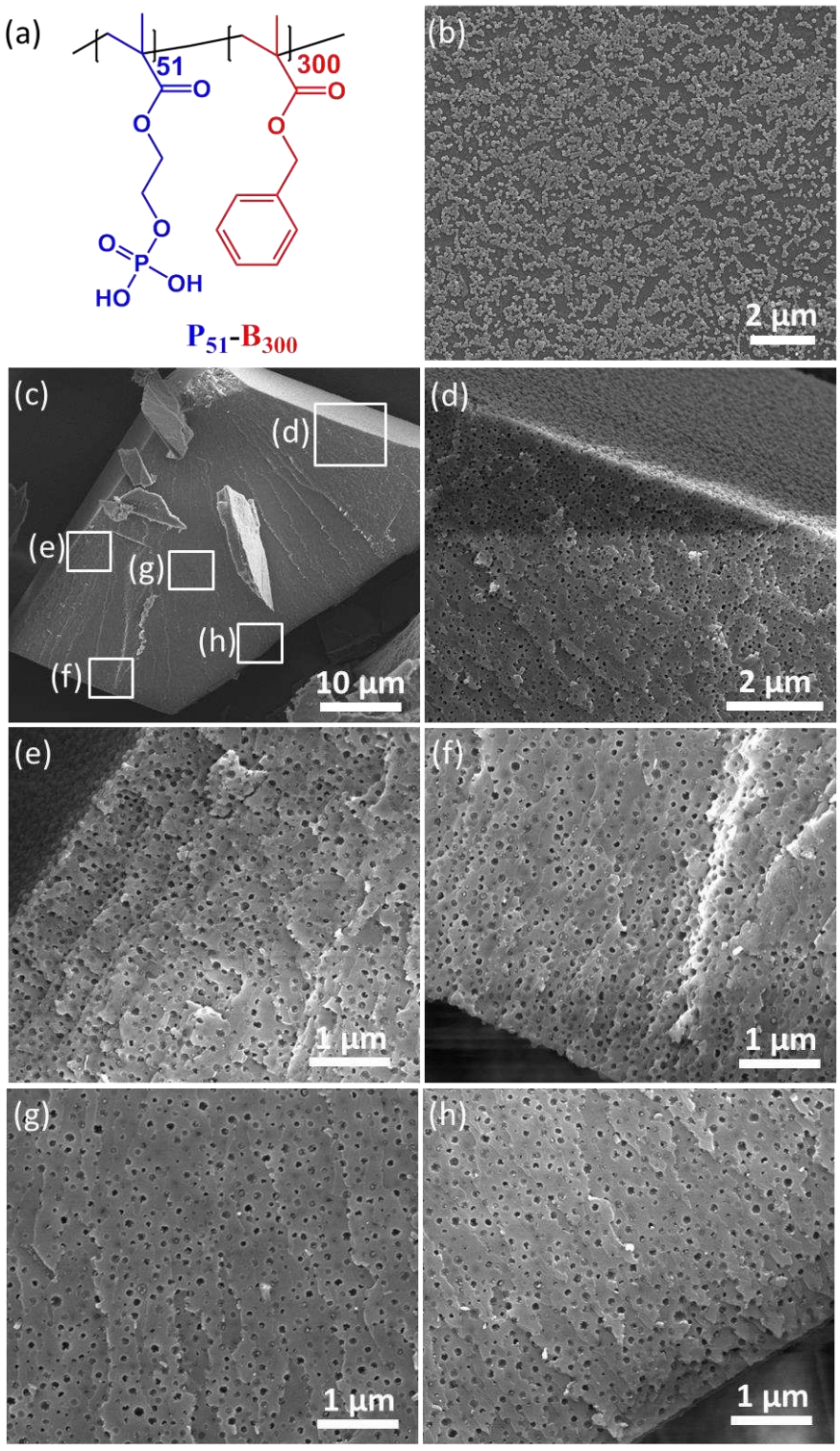

Figure S14. Occlusion of poly(2-(phosphonooxy)ethyl methacrylate)$_{51}$-poly(benzyl methacrylate)$_{300}$ (P_{51}-B_{300}) diblock copolymer nanoparticles within calcite crystals. (a) Chemical structure of P_{51}-B_{300} diblock copolymer nanoparticles; (b) SEM image recorded for P_{51}-B_{300} diblock copolymer nanoparticles; (c)-(h) SEM images showing the internal structure of a randomly-fractured calcite crystal precipitated in the presence of 0.1% w/w P_{51}-B_{300} diblock copolymer nanoparticles. Note: (d)-(h) are magnified SEM images, showing the corresponding areas indicated in (c). Clearly, uniform P_{51}-B_{300} diblock copolymer nanoparticle occlusion throughout the whole crystal is observed in this case. This demonstrates the generic nature of our findings.

References

(1) Semsarilar, M.; Jones, E. R.; Blanazs, A.; Armes, S. P. *Adv. Mater.* **2012**, *24*, 3378-3382.

(2) Couvreur, L.; Lefay, C.; Belleney, J.; Charleux, B.; Guerret, O.; Magnet, S. *Macromolecules* **2003**, *36*, 8260-8267.

(3) Ilavsky, J.; Jemian, P. R. *J. Appl. Cryst.* **2009**, *42*, 347-353.

(4) Pedersen, J. S. *J. Appl. Cryst.* **2000**, *33*, 637-640.

(5) Fielding, L. A.; Lane, J. A.; Derry, M. J.; Mykhaylyk, O. O.; Armes, S. P. *J. Am. Chem. Soc.* **2014**, *136*, 5790-5798.

(6) Lovett, J. R.; Derry, M. J.; Yang, P.; Hatton, F. L.; Warren, N. J.; Fowler, Patrick W.; Armes, S. P. *Chem. Sci.* **2018**, *9*, 7138-7144.

(7) Bang, J.; Jain, S.; Li, Z.; Lodge, T. P.; Pedersen, J. S.; Kesselman, E.; Talmon, Y. *Macromolecules* **2006**, *39*, 1199-1208.

(8) Pedersen, J. S. *J. Chem. Phys.* **2001**, *114*, 2839-2846.

(9) Feigin, L.; Svergun, D. I.; Taylor, G. W. In *Structure analysis by small-angle X-ray and neutron scattering*; Springer: Plenum Press: New York, 1987, p 25-55.

(10) Ning, Y.; Whitaker, D. J.; Mable, C. J.; Derry, M. J.; Penfold, N. J. W.; Kulak, A. N.; Green, D. C.; Meldrum, F. C.; Armes, S. P. *Chem. Sci.* **2018**, *9*, 8396-8401.